Article

Cell Reports

Dicer and Hsp104 Function in a Negative Feedback Loop to Confer Robustness to Environmental Stress

Graphical Abstract

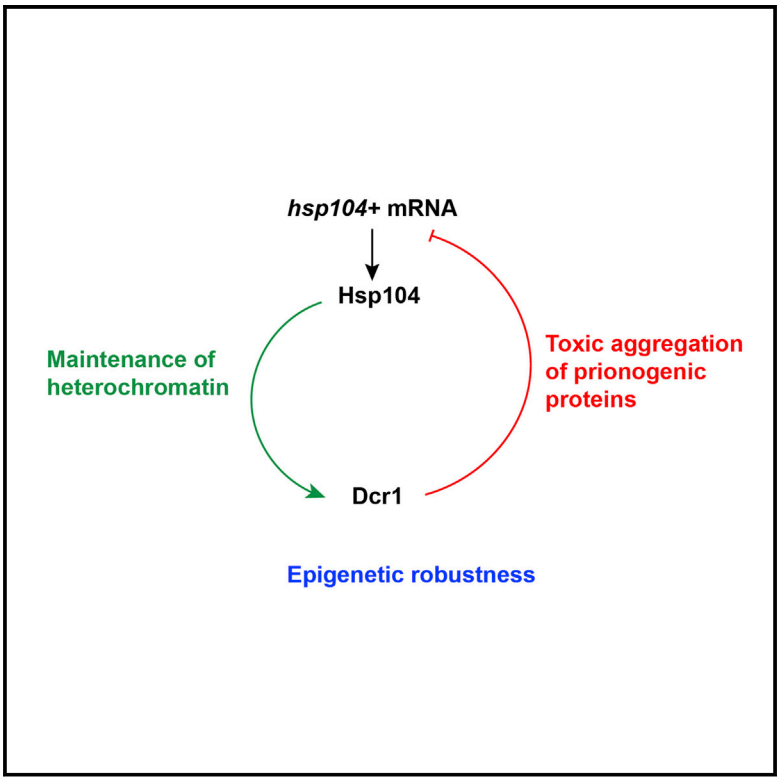

Authors

Daniele Oberti, Adriano Biasini, ..., Yukiko Shimada, Marc Bühler

Correspondence

marc.buehler@fmi.ch

In Brief

Environmental changes can impact epigenetic mechanisms and thus evoke phenotypic variation. In this study, Oberti et al. reveal a negative feedback loop involving the RNase Dicer and the protein disaggregase Hsp104 that buffers environmentally induced stochastic epigenetic variation and toxic aggregation of exogenous prionogenic proteins.

Highlights

- Dicer aggregates are recycled in a specialized cytoplasmic compartment
- Hsp104 and Dicer function in a negative feedback loop
- Hsp104 buffers environmentally induced epigenetic variation
- Dicer averts toxic aggregation of a prionogenic protein

Accession Numbers

GSE60640

Oberti et al., 2015, Cell Reports *10*, 47–61
January 6, 2015 ©2015 The Authors
http://dx.doi.org/10.1016/j.celrep.2014.12.006

Cell Reports
Article

Dicer and Hsp104 Function in a Negative Feedback Loop to Confer Robustness to Environmental Stress

Daniele Oberti,[1,2] Adriano Biasini,[1,2] Moritz Alexander Kirschmann,[1,2] Christel Genoud,[1,2] Rieka Stunnenberg,[1,2] Yukiko Shimada,[1,2] and Marc Bühler[1,2,*]
[1]Friedrich Miescher Institute for Biomedical Research, Maulbeerstrasse 66, 4058 Basel, Switzerland
[2]University of Basel, Petersplatz 10, 4003 Basel, Switzerland
*Correspondence: marc.buehler@fmi.ch
http://dx.doi.org/10.1016/j.celrep.2014.12.006

SUMMARY

Epigenetic mechanisms can be influenced by environmental cues and thus evoke phenotypic variation. This plasticity can be advantageous for adaptation but also detrimental if not tightly controlled. Although having attracted considerable interest, it remains largely unknown if and how environmental cues such as temperature trigger epigenetic alterations. Using fission yeast, we demonstrate that environmentally induced discontinuous phenotypic variation is buffered by a negative feedback loop that involves the RNase Dicer and the protein disaggregase Hsp104. In the absence of Hsp104, Dicer accumulates in cytoplasmic inclusions and heterochromatin becomes unstable at elevated temperatures, an epigenetic state inherited for many cell divisions after the heat stress. Loss of Dicer leads to toxic aggregation of an exogenous prionogenic protein. Our results highlight the importance of feedback regulation in building epigenetic memory and uncover Hsp104 and Dicer as homeostatic controllers that buffer environmentally induced stochastic epigenetic variation and toxic aggregation of prionogenic proteins.

INTRODUCTION

Epigenetics is the study of heritable changes in gene expression and phenotypic states that occur without a change in DNA sequence (Gottschling, 2004). Instead, chemical modifications such as methylation of DNA and histone proteins can act as epigenetic marks that stably affect gene expression and can be passed on to subsequent generations. Besides chromatin-dependent mechanisms, epigenetic information can also be transmitted by protein-based elements such as prions (Grossniklaus et al., 2013). Although epigenetic changes can be stably inherited, they are also reversible. Indeed, there can be considerable stochastic fluctuations between epigenetic states, which can potentially alter cellular and organismal phenotypes (Fraga et al., 2005; Wong et al., 2010).

Stochastic fluctuations between epigenetic states are thought to be mediated both by extrinsic and intrinsic factors. In particular, the impact of the environment on epigenetic genome regulation has attracted considerable interest. However, apart from a few well-studied natural processes such as vernalization whereby plants acquire the ability to flower in the spring upon cold exposure in winter (Song et al., 2013), it remains largely unknown if and how environmental cues like temperature trigger alterations in the epigenome (Feil and Fraga, 2011).

Heterochromatin also plays an essential role in epigenetic gene silencing in organisms ranging from yeast to humans. A classical example of heritable gene regulation mediated by heterochromatin is position effect variegation (PEV), a universally conserved epigenetic phenomenon where the expression of inserted or translocated genes is influenced by nearby heterochromatin. In *Schizosaccharomyces pombe*, genes placed within any of the three heterochromatic centromeres are repressed (Allshire, 1995; Allshire et al., 1994). However, the degree of repression depends upon the centromeric region. *S. pombe* centromeres are composed of a nonrepetitive central domain (*cnt*) around which outer repeat (*otr*) domains are symmetrically arranged (Chikashige et al., 1989). The *otr* domains are composed of *dg*/*dh* repeats that, like centromeres of higher eukaryotes, assemble into constitutive heterochromatin. Marker genes inserted into the *cnt* domain display a mosaic gene expression pattern reminiscent of PEV, whereas gene repression in the *otr* domain is remarkably strong without noticeable phenotypic variegation (Allshire et al., 1994; this study). Thus, the mechanisms that propagate the epigenetic state of the *otr* regions of *S. pombe* centromeres are highly effective.

Although it seems paradoxical, transcription of the *otr* region is necessary to stably propagate centromeric heterochromatin by a mechanism that engages the RNAi pathway (Castel and Martienssen, 2013). Indeed, centromeres of *S. pombe* cells with a nonfunctional RNAi pathway have severely impaired heterochromatin, causing chromosome segregation problems and derepression of centromeric sequences (Volpe et al., 2002, 2003).

Besides its critical role in the maintenance of centromeric heterochromatin, the *S. pombe* RNAi pathway also contributes to the tight repression of a class of euchromatic protein-coding genes referred to as "bound by Atf1 under normal conditions" (BANC) (Woolcock et al., 2012). BANCs are stress-response genes such as those encoding heat shock proteins that are

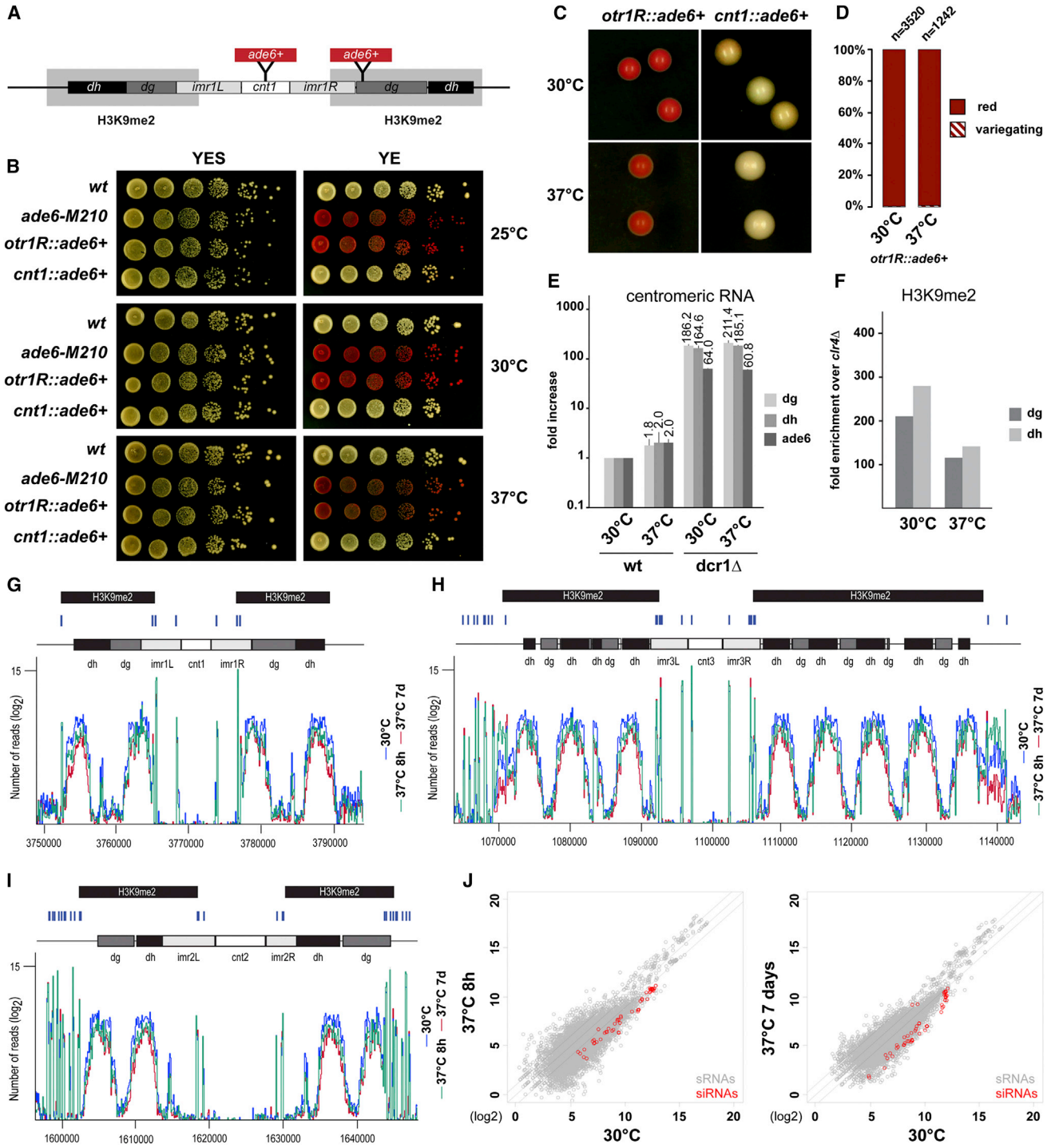

Figure 1. Centromeric Silencing Is Maintained at Elevated Temperatures

(A) Schematic of the centromeric region of chromosome I, highlighting the positions of the *ade6+* reporter used in (B) and (C).

(B) Silencing assays of strains bearing the *ade6+* reporter grown on YES and YE plates. The *otr1R*::*ade6+* reporter reveals robust silencing at all temperatures tested.

(C) Imaging of single colonies showing robust silencing of the *otr1R*::*ade6+* reporter at 30°C and 37°C, in contrast to slight silencing of the *cnt1*::*ade6+* reporter at 30°C and loss of silencing at 37°C.

(D) Phenotypic assessment of single colonies of *otr1R*::*ade6+* cells.

(E) Quantitative RT-PCR of centromeric (*dg*/*dh*) and *ade6+* transcripts showing robust silencing at 37°C in *WT* cells. In contrast, silencing is lost in *dcr1Δ* cells. Levels are normalized to *WT* cells at 30°C and *act1+* RNA.

(legend continued on next page)

constitutively bound by the transcriptional activator Atf1 (Kon et al., 1997). Upon stress, Atf1 is rapidly phosphorylated and causes strong transcriptional activation of most of its target genes (Lawrence et al., 2007). Under nonstressful conditions, the RNAi factor Dicer (Dcr1) colocalizes with BANCs at nuclear pores, contributing to their firm repression presumably by degrading nascent transcripts (Woolcock et al., 2012).

Dcr1 localization and activity is regulated in a unique temperature-dependent manner. Under normal conditions in *S. pombe*, Dcr1 is predominantly nuclear (Emmerth et al., 2010), but upon acute thermal stress, it accumulates in large cytoplasmic foci. This is controlled by the double-stranded RNA-binding domain (dsRBD) of Dcr1: proper folding of the dsRBD is required for nuclear retention of Dcr1, whereas unfolding of the dsRBD and thus loss of nuclear retention can be induced by temperatures above 34°C. In vitro, these high temperatures cause precipitation of the dsRBD and progressive loss of nuclear magnetic resonance signals, indicative of protein aggregation. Thus, the Dcr1 dsRBD constitutes a thermoswitch that controls conditional relocalization of Dcr1 and may render Dcr1 aggregation prone above 34°C (Barraud et al., 2011; Woolcock et al., 2012).

Temperature-induced loss of nuclear-pore-associated Dcr1 provides an elegant mechanism for the release of BANC genes from RNAi repression under temperature stress (Holoch and Moazed, 2012). However, it raises two important questions: how is aggregation of Dcr1 prevented and, given the loss of nuclear Dcr1, what ensures the integrity of centromeric heterochromatin at elevated temperatures? Furthermore, the physiological relevance of Dcr1-mediated BANC repression has remained elusive. Here, we demonstrate that resilience of centromeric heterochromatin critically depends on Hsp104, a protein disaggregase that dissolves Dcr1 aggregates at elevated temperatures. The BANC gene *hsp104+* itself is negatively regulated by Dcr1, which averts the toxic aggregation of a budding yeast prion protein.

RESULTS

Silencing within Constitutive Heterochromatin Is Temperature Insensitive

To investigate the robustness of centromeric heterochromatin to temperature variations, we used *S. pombe* strains in which *ade6+* reporter genes were either inserted into the central core domain *cnt1* (*cnt1*::*ade6+*) or the juxtaposed heterochromatic *dg/dh* region (*otr1*::*ade6+*; Figure 1A). In this assay, wild-type (*WT*) cells form white colonies, whereas cells with a nonfunctional *ade6-M210* allele give rise to red colonies under limiting adenine conditions (Figure 1B). *cnt1*::*ade6+* cells formed mostly white colonies at 30°C with low degrees of redness at lower temperatures and pure white color at 37°C (Figures 1B and 1C). This is consistent with reports that variegated expression of genes in *cnt* regions is sensitive to temperature changes (Allshire et al., 1994). In contrast, *otr1*::*ade6+* cells gave rise to dark red colonies at all temperatures (Figures 1B–1D). Thus, the *ade6+* gene placed within constitutive heterochromatin is strongly repressed and exhibits negligible phenotypic variation even when exposed to higher temperatures.

To assess repression of the *dg/dh* repeats in the heterochromatic *otr1* region directly, we measured *dh* and *dg* RNA levels by quantitative RT-PCR. In *dcr1Δ* cells, which have impaired heterochromatin formation, *dg/dh* RNA levels typically increase more than 100-fold. However, when *otr1*::*ade6+* cells were grown at 37°C, *dg* and *dh* RNA levels increased by only 2-fold compared to the same cells grown at 30°C (Figure 1E). Thus, consistent with the previous result, silencing of heterochromatin is not greatly affected at 37°C. Moreover, when cells were grown at 37°C, H3K9me2, a hallmark of heterochromatin, was largely maintained at both *dg* and *dh* repeats (Figure 1F), and there were no major defects in chromosome segregation, which also requires heterochromatic structures.

These results demonstrate that centromeric heterochromatin in *S. pombe* is temperature insensitive. This is in stark contrast to the repression of genes placed at the *cnt* domain of centromeres, which is completely abrogated at temperatures above 30°C.

Dcr1 Is Required for Repression of Centromeric Heterochromatin at Elevated Temperatures

A functional RNAi pathway is essential for silencing centromeric heterochromatin and maintaining high H3K9me2 levels (Volpe et al., 2002). It has been suggested that RNAi in *S. pombe* could be suppressed at higher temperatures (Kloc et al., 2008). In addition, we previously showed that, at elevated temperatures, Dcr1 translocates from the nucleus to the cytoplasm and speculated that this would abrogate the repressive activity of Dcr1, at least for BANC genes (Woolcock et al., 2012). Under these assumptions, RNAi would be expected to be dispensable for heterochromatin silencing at 37°C. However, we observed a dramatic increase in *dg/dh* transcript levels at both 30°C and 37°C upon deletion of the *dcr1+* gene (Figure 1E), demonstrating that Dcr1 is required for repression of heterochromatin also at elevated temperatures.

Dcr1 is thought to act on chromatin to cleave double-stranded RNA into short interfering RNAs (siRNAs) (Emmerth et al., 2010; Woolcock et al., 2011, 2012). Thus, the observed requirement of Dcr1 for silencing also at 37°C implies continuous generation of siRNAs. Consistent with this, deep sequencing of total small RNA libraries revealed highly abundant siRNAs also at 37°C. Although we observed a slight reduction of siRNAs at 37°C (Figure 1J), they remained high even when cells were grown at 37°C for several days (Figures 1G–1I). From these results, we conclude that siRNA biogenesis or stability is not greatly affected at elevated temperatures in *S. pombe*.

(F) ChIP experiment showing only moderate decrease of H3K9me2 enrichment at centromeric *dg* and *dh* repeats upon exposure to 37°C. The value for *clr4Δ* cells was set to 1 and fold enrichment normalized to *adh1+*.

(G–I) Small RNA reads mapping to the centromeres of the three chromosomes (G: chromosome I; I: chromosome II; H: chromosome III). Small RNAs were collected from samples grown at 30°C and from samples shifted to 37°C for 8 hr and 7 days.

(J) Scatterplot of siRNA peaks (red) and total small RNA (sRNA) peaks (gray) in cells grown at 30°C versus cells shifted to 37°C for 8 hr (left) or 7 days (right).

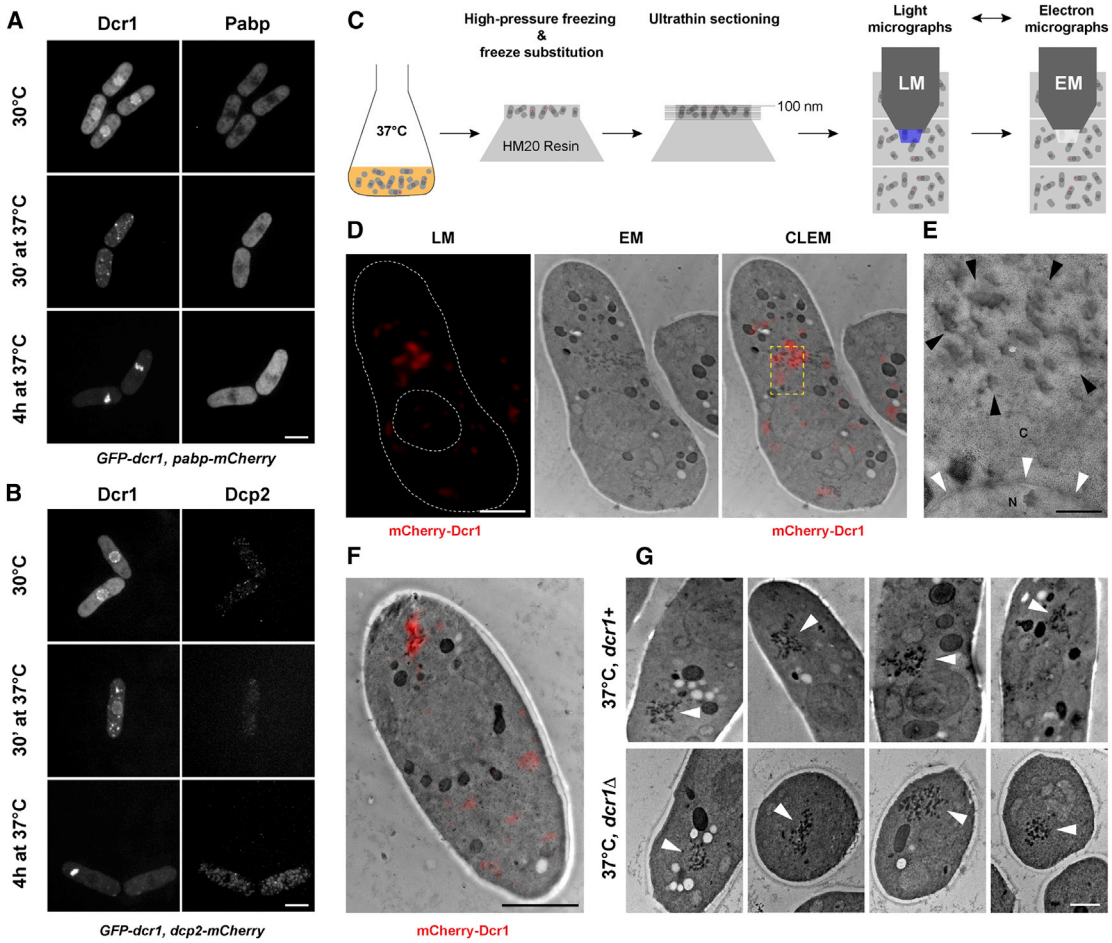

Figure 2. Dcr1 Accumulates in Electron-Dense Cytoplasmic Inclusions at Elevated Temperatures

(A) Two-color live imaging of GFP-Dcr1- and Pabp-mCherry-expressing cells at different conditions reveals no specific colocalization of the two proteins. The scale bar represents 5 μm.

(B) Two-color live-cell imaging of GFP-Dcr1 and Dcp2-mCherry. The scale bar represents 5 μm.

(C) Schematic of the correlative microscopy workflow, in which the same ultrathin sections are imaged by light and transmission electron microscopy.

(D) Correlative microscopy of Dcr1 localization during heat stress. The scale bar represents 1 μm. LM, light microscopy.

(E) Enlargement of the region highlighted in (D), where Dcr1 is localized in electron-dense particles (black arrows). The nuclear envelope is also clearly visible thanks to high ultrastructure preservation (white arrows). The scale bar represents 200 nm.

(F) Another example showing Dcr1 localization in electron-dense particles. The scale bar represents 1 μm.

(G) Imaging of electron-dense particles (white arrows) in *dcr1+* and *dcr1Δ* cells at 37°C. The scale bar represents 1 μm.

Dcr1 Accumulates in Electron-Dense Cytoplasmic Inclusions at Elevated Temperatures

Thus far, we have shown that Dcr1 is required for repression of genes in the heterochromatic *otr* region of centromeres also at higher temperatures. Given that we previously observed Dcr1 accumulating in cytoplasmic foci at elevated temperatures (Woolcock et al., 2012), we further explored the nature of these cytoplasmic Dcr1 bodies (Figures 2A and 2B). As described previously, endogenous Dcr1 levels are not detectable by fluorescence microscopy (Emmerth et al., 2010). Therefore, similar to previous experiments, we used strains expressing Dcr1 to a level sufficient for detection by fluorescence microscopy (Emmerth et al., 2010; Barraud et al., 2011; Woolcock et al., 2012). We note that these conditions reflect physiological Dcr1 localization as assessed by other methods that do not rely on overexpression (Woolcock et al., 2012).

The formation of cytoplasmic structures is commonly observed when eukaryotic cells are exposed to nonphysiological growth temperatures. Under severe heat stress, general repression of translation causes a redistribution of mRNAs into stress granules (SGs) (Anderson and Kedersha, 2006). In *S. pombe*, SGs form when cells are exposed to 42°C (Dunand-Sauthier et al., 2002). Consistent with this, we did not observe formation of SGs at 37°C (Figure 2A). However, cytoplasmic Dcr1 bodies formed after only 30 min exposure to 37°C (Figures 2A and 2B). Thus, Dcr1 does not localize to SGs under mild temperature stress.

In mammalian cells, many RNAi factors can be found in processing bodies (P bodies), prompting us to look for a possible

colocalization of Dcr1 with P bodies. Unlike SGs, P bodies exist even under nonstress condition (Mollet et al., 2008). Indeed, Dcp2-mCherry, a P body marker, showed punctate staining already at 30°C. Importantly, Dcr1 did not colocalize with Dcp2 either at 30°C or at 37°C (Figure 2B). Thus, the cytoplasmic Dcr1 bodies that form under mild heat stress are not SGs or P bodies.

To obtain more conclusive information about the precise cytoplasmic localization of Dcr1, we implemented correlative light and electron microscopy (CLEM). CLEM overcomes several limitations of light microscopy for analyzing the localization of fluorescently labeled proteins by combining it with electron microscopy (EM) to allow for higher resolution and to reveal the context where the protein of interest is located. The protocol we used is based on cell cryofixation, followed by freeze substitution and embedding in a Lowicryl resin, and ensures preservation of both fluorescent signal and ultrastructure as well as straightforward correlation of the two data sets (Figure 2C; Kukulski et al., 2011). In addition, by imaging sections with a thickness below the axial resolution of classical light microscopy, a higher z resolution is achieved than with confocal microscopy (Micheva and Smith, 2007).

We sequentially imaged ultrathin (<200 nm) sections from mCherry-Dcr1-expressing cells exposed for 4 hr to 37°C in a light microscope and in a transmission EM (Figure 2C). As expected from the confocal live imaging, we detected strong fluorescent mCherry-Dcr1 signal mostly in a single cytoplasmic region in every cell (Figure 2D). The signal obtained from imaging ultrathin sections however was less homogenous than whole-cell live imaging and distributed in small patches, a difference possibly due to the increased resolution. Interestingly, imaging of the same ultrathin sections in the EM and superposition of the light and electron micrographs revealed that the fluorescent signal corresponds to a cytoplasmic structure not previously described in *S. pombe* (Figures 2D–2F). This structure comprises smaller electron-dense cytoplasmic accumulations, not enclosed by membranes (Figure 2E). This structure was not observed in cells grown at 30°C but was highly characteristic of cells exposed to 37°C (Figure 2G). Moreover, these structures also formed in the absence of Dcr1 (Figure 2G). Thus, thermal stress provokes the formation of distinct electron-dense structures in the cytoplasm, in which Dcr1 accumulates during the acute phase of the stress.

Dcr1 Colocalizes with the Protein Disaggregase Hsp104 in Cytoplasmic Inclusions

The CLEM experiments were conducted on single ultrathin sections, which cover only a small cell subvolume, hindering an assessment of the number and distribution of the observed inclusions. We therefore imaged cells in their entirety using serial block-face electron microscopy (SBEM), a method that allows automated 3D imaging by combining block-face imaging with serial sectioning in a scanning EM (Denk and Horstmann, 2004). We acquired a volume encompassing several cells that had been exposed to 37°C for 4 hr before fixation and embedding. We found the electron-dense inclusions to be mostly concentrated in one region in the cytoplasm (Figures 3A, 3B, and S1; Movie S1), even in dividing cells (Figures 3C, 3D, and S1; Movie S2). 3D reconstruction confirmed that this structure is composed of many small accumulations of electron-dense material (interactive 3D model in Figure S2). In the case of the cell in Figure 3A, the cluster of electron-dense patches had a volume of around 2% of the total cell volume, but only 1/3 of it was electron dense. In this preparation, in which membranes are well stained, we again did not observe membranes enclosing the inclusion (Figures 3B and 3D).

The temperature-stress-induced electron-dense inclusions that we observed are reminiscent of heat-dependent electron-dense patches that have been associated with the protein disaggregase Hsp104 in *S. cerevisiae* (Fujita et al., 1998; Kawai et al., 1999). Hsp104 is a hexameric AAA+ ATPase that couples ATP hydrolysis to protein disaggregation (Doyle et al., 2013; Vashist et al., 2010). It mediates the resolubilization of heat-inactivated proteins from insoluble aggregates and plays an essential role in induced thermotolerance and prion propagation (Glover and Lindquist, 1998; Parsell et al., 1994; Sanchez and Lindquist, 1990). Therefore, we investigated Hsp104-mCherry localization in *S. pombe*. As observed for mCherry-Dcr1, Hsp104-mCherry accumulated in bright cytoplasmic foci at 37°C. Moreover, CLEM imaging revealed that the fluorescent Hsp104 signal corresponds to the same non-membrane-enclosed electron-dense cytoplasmic inclusion as described above (Figure 3E). Finally, labeling of Dcr1 and Hsp104 with two different fluorescent tags revealed perfect cytoplasmic colocalization of the two proteins at 37°C (Figures 3F and 3G).

Hsp104 Is Necessary to Dissolve Cytoplasmic Dcr1 Aggregates

The above results strongly suggested that the electron-dense material that we observed in the cytoplasm of cells that have been exposed to mild heat stress represent protein aggregates. Unlike most ''canonical'' heat shock proteins, Hsp104 disaggregates and remodels a broad repertoire of aggregated and unfolded proteins (DeSantis et al., 2012; Parsell et al., 1994). Consistent with this, we observed that the electron-dense inclusions visible during acute temperature stress progressively disappeared upon prolonged exposure to 37°C. However, they persisted in cells lacking Hsp104 (Figure 4A). We also observed a concomitant disappearance of the Hsp104-mCherry signal over time (Figures 4B and 4C). Therefore, the electron-dense cytoplasmic compartment that forms at 37°C and contains Dcr1 is likely the site where Hsp104 reactivates heat-denatured proteins.

Because we observed Hsp104 and Dcr1 colocalizing in the electron-dense cytoplasmic inclusions, we speculated that the fluorescent Dcr1 bodies observed at elevated temperatures represent aggregates of unfolded Dcr1 protein that eventually get resolubilized by Hsp104. Consistent with this compartment containing aggregated, insoluble Dcr1 molecules, fluorescence recovery after photobleaching (FRAP) experiments revealed that Dcr1 in this structure is immobile (Figure 4D). To directly test whether Hsp104 disaggregates Dcr1, we shifted cells grown at 30°C to 37°C and monitored the presence of Dcr1 aggregates in *hsp104+* and *hsp104Δ* cells over time by light microscopy (Figures 4B and 4E). In *WT hsp104+* cells, we observed the formation of a high number of small cytoplasmic Dcr1 foci during the first

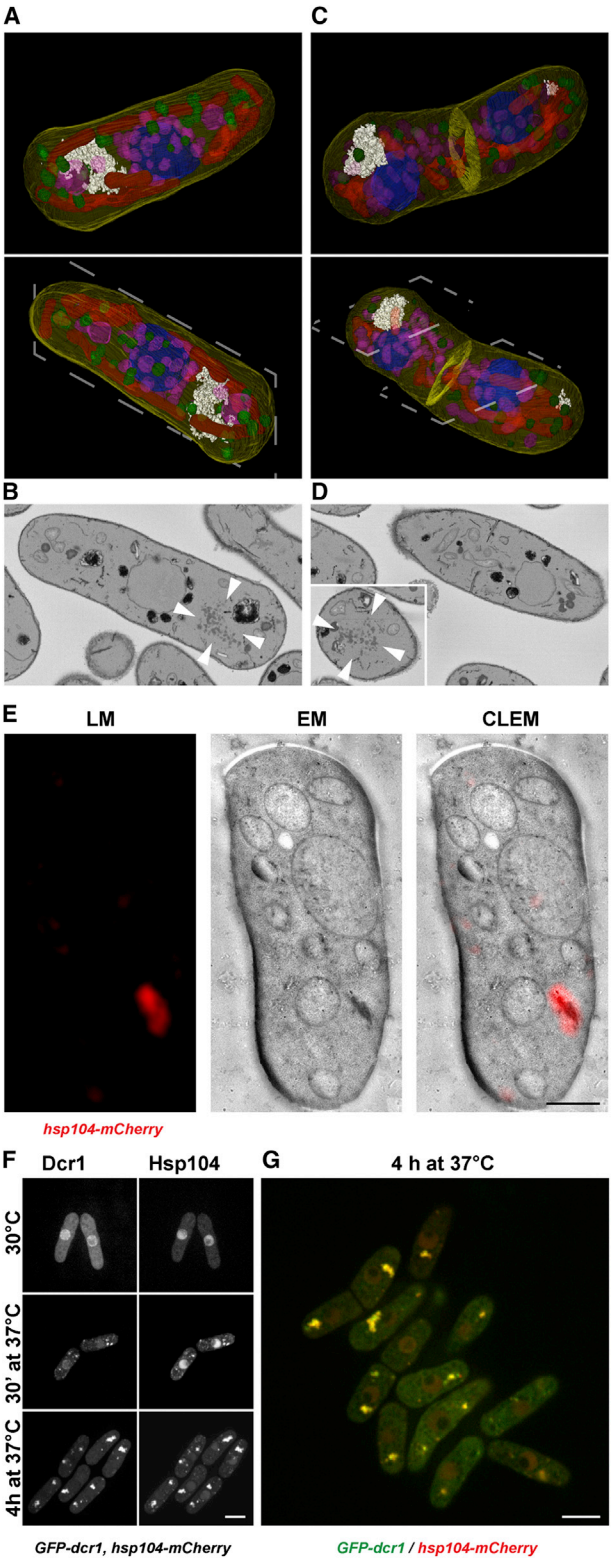

Figure 3. Dcr1 Colocalizes with Hsp104 in Electron-Dense Inclusions

(A) Reconstruction of *S. pombe* cell based on serial block-face electron microscopy imagery. White, electron-dense inclusions; blue, nucleus; red, mitochondria; pink and green, vesicles; gray dashed line, sectioning plane for (B).

(B) EM section through the cell reconstructed in (A). White arrows, electron-dense inclusion.

(C) Reconstruction of a cell undergoing mitosis. Color code as in (A); the septum is additionally shown in yellow.

(D) EM sections through the cell reconstructed in (C).

(E) Correlative microscopy imaging of hsp104-mCherry-expressing cell. The scale bar represents 1 μm.

(F) Two-color live-cell imaging of GFP-Dcr1 and hsp104-mCherry. The scale bar represents 5 μm.

(G) Two-color live-cell imaging of GFP-Dcr1 (green) and hsp104-mCherry (red). The scale bar represents 5 μm.

hour of heat stress. These then clustered in one or two large aggregates after 3 hr and subsequently disappeared progressively (Figures 4E and 4F). We also observed a high number of small Dcr1 foci during acute heat stress in *hsp104*Δ cells. These also clustered into one or two large aggregates after 3 hr, but, in contrast to the *WT* cells, they were significantly larger in size and tended to become even bigger during prolonged heat stress rather than disappearing (Figures 4E and 4F). Thus, the cytoplasmic Dcr1 bodies that form during the acute phase of temperature stress represent immobile, aggregated Dcr1 proteins, which become progressively disaggregated by Hsp104.

Recycling of Resolubilized Dcr1

Protein quality-control systems have evolved in all life kingdoms to prevent protein aggregation by facilitating either folding and refolding of misfolded proteins or their removal by proteolytic degradation (Goldberg, 2003; Tyedmers et al., 2010a). To investigate whether aggregated Dcr1 undergoes proteolysis or whether it can be properly refolded and return to the nucleus, we grew cells at 37°C for 4 hr, shifted them back to 30°C, and imaged GFP-tagged Dcr1 (Figure 5A). Similar to the result with chronic heat stress, cytoplasmic Dcr1 aggregates gradually disappeared in *WT* cells, whereas in *hsp104Δ* cells, the Dcr1 aggregates persisted during recovery (Figures 5B and 5C). Importantly, the nuclear localization of Dcr1 was rapidly restored in both *hsp104*+ and *hsp104*Δ cells during recovery from heat stress (Figure 5B). To find out whether this nuclear pool of Dcr1 is exclusively newly synthesized protein or whether disaggregated Dcr1 also contributes to replenishing it, we imaged cells in which protein synthesis was blocked with cycloheximide during the recovery phase (Figure 5A). Under these conditions, nuclear Dcr1 localization was readily restored in *hsp104*+ cells, but not in *hsp104*Δ cells (Figures 5D and 5E). When we photobleached Dcr1 fluorescence at the onset of recovery (Figure 5A), we could not detect any fluorescence during recovery, demonstrating that there was no new synthesis of Dcr1 protein during the course of this experiment (Figure 5D).

Thus, in the presence of Hsp104, aggregated cytoplasmic Dcr1 can be resolubilized and properly folded to re-enter the nucleus.

Hsp104 Confers Epigenetic Robustness at Elevated Temperatures

The foregoing results indicated that Hsp104 could be required to prevent loss of heterochromatin at elevated temperatures by

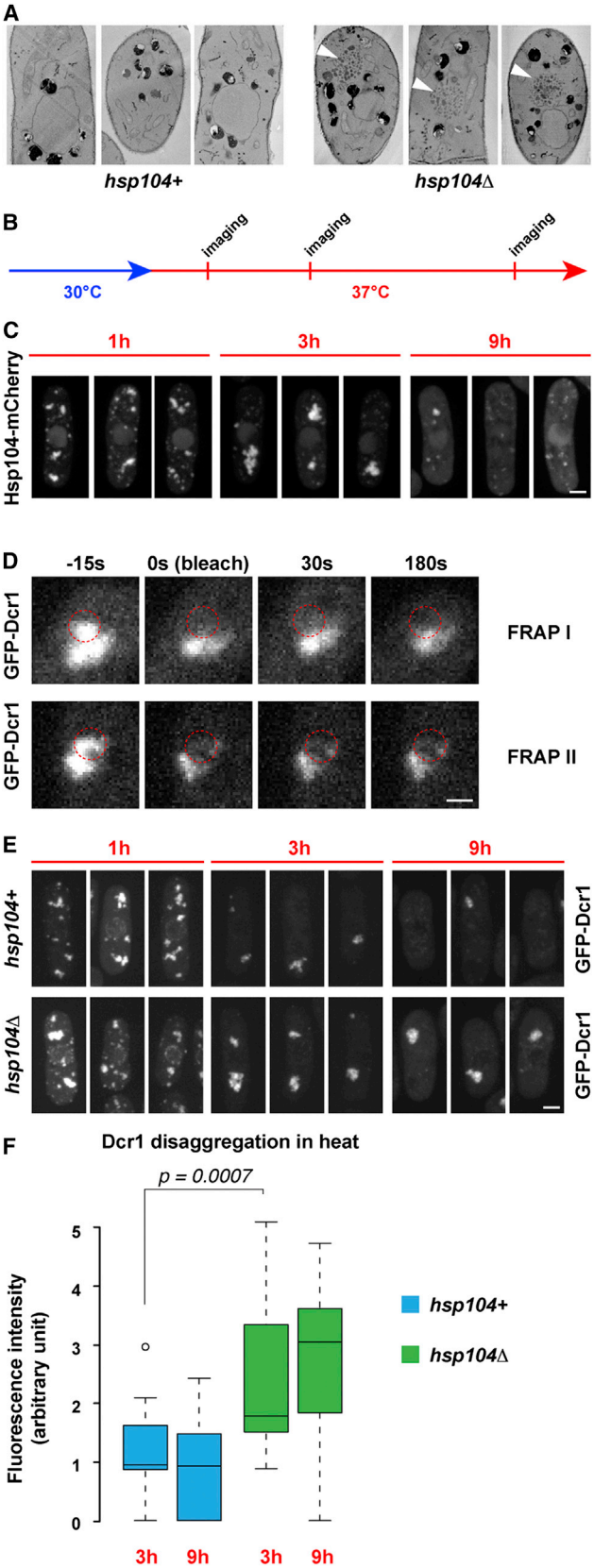

Figure 4. Disaggregation of Dcr1 Bodies Depends on Hsp104

(A) Electron microscopy imaging of *hsp104+* and *hsp104Δ* cells grown at 37°C for 10 hr. White arrows, electron-dense inclusions.

(B) Schematic of the experiment shown in (C). Cells were exposed to heat and imaged at different time points.

(C) Live-cell imaging of Hsp104-mCherry-expressing cells exposed to heat. The scale bar represents 2 μm.

(D) FRAP of GFP-Dcr1 foci. Images were acquired at the indicated time points. Two representative images are shown. Red, photobleached region. The scale bar represents 1 μm.

(E) Live-cell imaging of GFP-Dcr1 fluorescence of *hsp104+* and *hsp104Δ* cells exposed to heat. The scale bar represents 2 μm.

(F) Quantification of fluorescence in aggregates in *hsp104+* and *hsp104Δ* cells.

sustaining a sufficient amount of functional Dcr1 protein. Indeed, we observed that the repression of the heterochromatic *otr1*::*ade6+* gene became unstable in *hsp104*Δ cells at 37°C (Figures 6A and 6B). Specifically, rather than an overall loss of silencing in the entire population of cells, we observed switching between repressed and derepressed states of the *otr1*::*ade6+* gene. When we plated *hsp104*Δ cells and grew them at 37°C, we observed colonies with red and white sectors (Figure 6A). Such variegated expression of the *otr1*::*ade6+* gene hardly occurs at 30°C in either *WT* or *hsp104*Δ cells (Figures 1D and 6B). However, this phenotype was very pronounced at 37°C in *hsp104*Δ cells (Figure 6B). Notably, variegating colonies showed either fully white or dark red sectors, demonstrating that no intermediate *ade6+* expression states were established. Rather, the *otr1*::*ade6+* gene is either switched on or off in *hsp104*Δ cells at 37°C. Because all cells are genetically identical, this switch is of an epigenetic nature, and we therefore refer to *otr1*::*ade6+* "*on*" or "*off*" epialleles.

The formation of white sectors (i.e., *otr1*::*ade6+* "*on*") in *hsp104*Δ colonies indicated that thermal stress could cause a loss of heterochromatin in the absence of Hsp104. Indeed, we observed drastically reduced, yet not completely abolished, H3K9me2 levels on centromeric repeats in *hsp104*Δ cells that were grown at 37°C (Figure 6C). This experiment can only be performed with a mixed population of variegating cells, so it is possible that H3K9me2 levels are completely abolished in certain cells. Because we could not determine H3K9me2 levels on a single-cell level, we instead monitored chromosome segregation, which also requires functional heterochromatin, at the single-cell level in *hsp104Δ* cells by microscopy. Mutations that disrupt centromeric heterochromatin result in elevated rates of chromosome loss and nonsegregated, lagging chromosomes in late anaphase (Ekwall et al., 1999). We did not observe abnormal chromosome segregation patterns in *WT* cells grown at 37°C. However, we did observe lagging chromosomes in *hsp104Δ* cells at 37°C (Figure 6D). These results reveal that Hsp104 confers epigenetic robustness to *S. pombe* cells at elevated temperatures. In addition, lack of Hsp104 activity at elevated temperatures not only impacts heterochromatic gene silencing but also compromises genome stability.

Inheritance of an Environmentally Induced Epigenetic Switch

The *otr1*::*ade6+-off* epiallele was remarkably stable at both 30°C and 37°C in *WT* cells and at 30°C in *hsp104*Δ cells. However, an

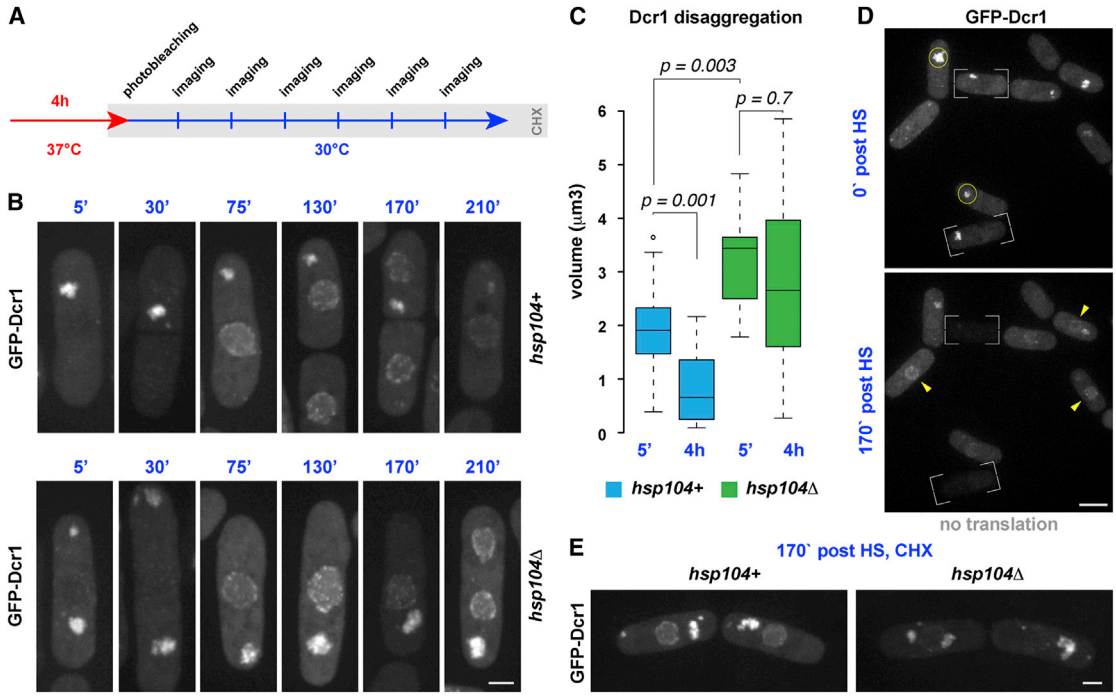

Figure 5. Disaggregated Dcr1 Re-enters the Nucleus

(A) Schematic of the experiment shown in (B). Cells pre-exposed to heat for 4 hr were shifted to 30°C and imaged at different time points.

(B) Live-cell imaging of *hsp104+* and *hsp104Δ* cells expressing GFP-Dcr1 recovering from heat condition. Different cells are shown at different time points. The scale bar represents 2 μm.

(C) Quantification of the size of GFP-Dcr1 aggregates during recovery.

(D) Live-cell imaging of *hsp104+* cells recovering from heat condition in the presence of cycloheximide. Control cells (white frames) were photobleached to confirm protein translation block. Nuclear signal is recovering after 170 min (yellow arrows), whereas cytoplasmic foci disappear (yellow circles). The scale bar represents 5 μm. HS, heat shock.

(E) Comparison of nuclear recovery in *hsp104+* and *hsp104Δ* cells treated with cycloheximide. The scale bar represents 2 μm.

increase in temperature to 37°C in *hsp104*Δ cells resulted in an unstable *otr1*::*ade6+* locus that displayed alternative silenced (*otr1*::*ade6+-off*) and expressed (*otr1*::*ade6+-on*) epigenetic states. Importantly, the *otr1*::*ade6+-on* epiallele was propagated for several cell divisions when *hsp104*Δ cells were grown at 37°C, as evidenced by the formation of white sectors within a given yeast colony (Figure 6A). Because *hsp104*Δ cells can restore the pool of functional Dcr1 by newly synthesized protein when shifted back to 30°C (Figure 5B), we predicted a rapid switch from the *otr1*::*ade6+-on* to the *otr1*::*ade6+-off* epiallele when temperature is reduced to 30°C. To test this, we selected variegating colonies at 37°C, grew them in two separate liquid cultures for about 14 divisions at 30°C or 37°C, and subsequently plated these cells to assess the epigenetic state of the *otr1*::*ade6+* allele (Figure 6E). As anticipated, we observed fully red (off) but rarely fully white (on) colonies at both temperatures, demonstrating that the *otr1*::*ade6-on* epiallele is less stable than the *otr1*::*ade6+-off* epiallele. Unexpectedly, however, we still observed a high number of white sectored colonies, although these cells had gone through at least 30 divisions at 30°C (Figure 6F). Once re-established, the *otr1*::*ade6+-off* epiallele was stably maintained (Figure S3). Thus, the *otr1*::*ade6-on* epiallele can be propagated for many divisions even in the absence of the thermal stress that initially induced the change in expression of the *otr1*::*ade6+* gene.

These results highlight that *hsp104+* mutants are predisposed to undergo temperature-induced, heritable changes in heterochromatic gene expression and reveal a phenomenon that complies with the classical definition of epigenetics (Gottschling, 2004; Ptashne, 2013).

Hsp104 and Dcr1 Function in a Negative Feedback Loop

Besides centromeric repeats, Dcr1 also physically associates with a group of stress-response genes referred to as BANCs (Woolcock et al., 2012). Under noninduced conditions, Dcr1 degrades BANC gene mRNAs cotranscriptionally, thereby assuring tight repression. Intriguingly, *hsp104+* is a BANC gene, and we have previously suggested that temperature-induced translocation of Dcr1 to the cytoplasm abrogates the repressive activity of Dcr1 on BANC gene expression (Woolcock et al., 2012).

To determine the influence of Dcr1 on the *hsp104+* expression dynamics with high temporal resolution, we measured the relative abundance of *hsp104+* mRNA in *WT* and *dcr1*Δ cells every 15 min for 3 hr, at 30°C and 37°C (Figure 7A). As expected, steady-state *hsp104+* mRNA levels were about 5- to 10-fold

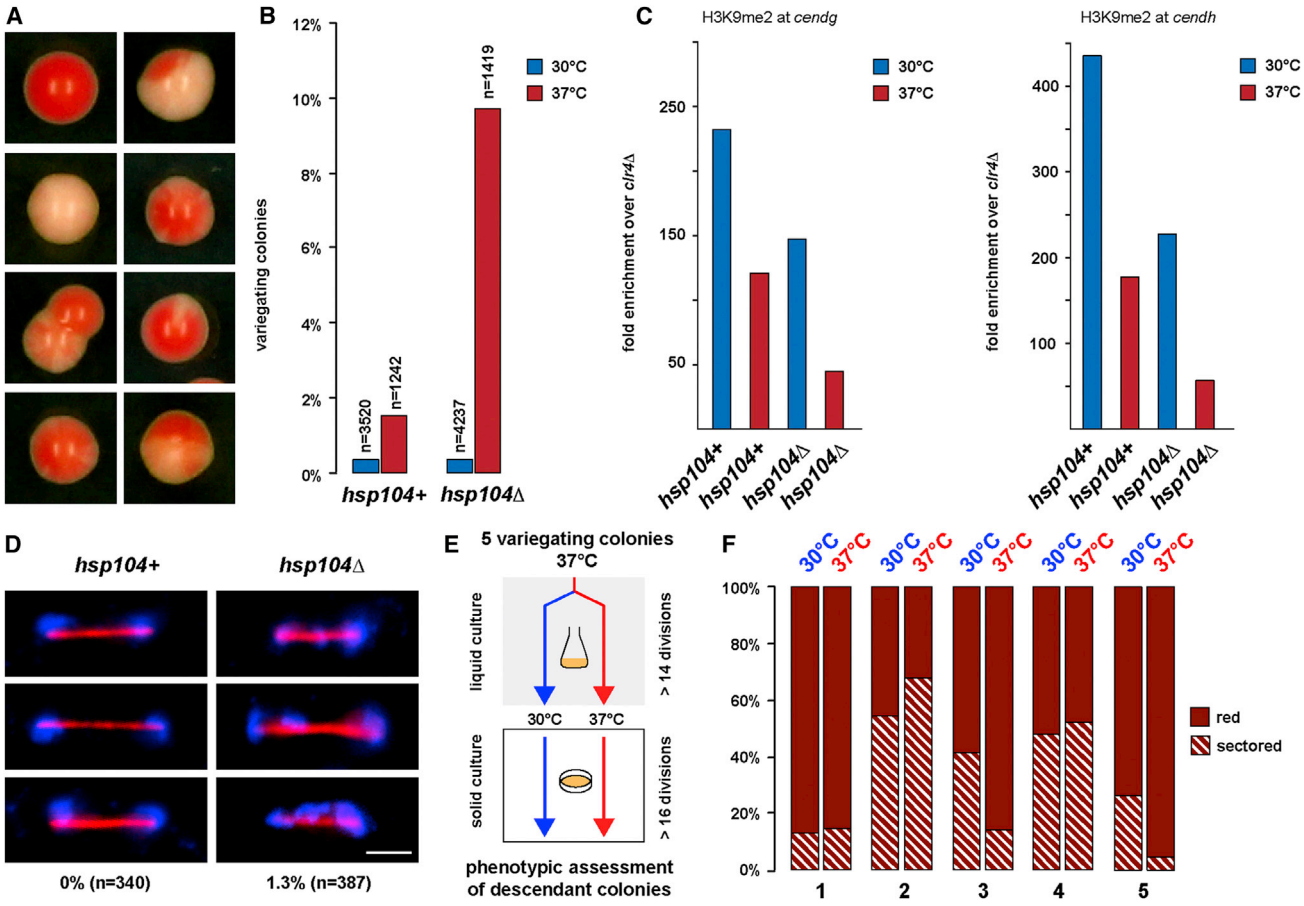

Figure 6. Hsp104 Confers Epigenetic Robustness

(A) Examples of *hsp104Δ* cells with *otr1R*::*ade6+* reporter showing a variegating phenotype after growth at 37°C.

(B) Assessment of variegation phenotype in *hsp104+* and *hsp104Δ* cells grown at 30°C and 37°C.

(C) ChIP experiment showing decreased H3K9me2 enrichment at centromeric (cen) *dg* and *dh* repeats in *hsp104Δ* cells at 37°C. The value for *clr4Δ* cells was set to 1 and fold enrichment normalized to *adh1+*.

(D) Lagging chromosomes in *hsp104Δ* cells. Cells grown at 37°C were stained with DAPI (blue) and α-tubulin (red). The scale bar represents 2.5 μm.

(E) Schematic of the experiment shown in (F). Variegating *hsp104Δ* colonies at 37°C were selected and further grown at 30°C or 37°C.

(F) Assessment of variegating phenotype of colonies originating from a variegating colony. Five representative examples are shown.

higher in *dcr1*Δ cells compared to *WT* cells at 30°C. When cells were shifted from 30°C to 37°C, we observed a rapid increase in *hsp104+* expression, reaching maximal levels 30 min after the temperature shift, in both *WT* and *dcr1Δ* cells. Surprisingly, rather than constantly high or steadily decaying *hsp104+* mRNA levels, we observed pulsatile expression patterns of *hsp104+* when *WT* and *dcr1*Δ cells were continuously grown at 37°C. The *hsp104+* gene cycled with a period length of approximately 30 min and synchronously in *WT* and *dcr1*Δ cells. However, *WT* cells displayed less-pronounced expression peaks than *dcr1*Δ cells, indicating that Dcr1 can still repress expression of the *hsp104+* gene at high temperatures. Except for the first expression maximum that was similar in *WT* and *dcr1*Δ cells in most experiments, *hsp104+* mRNA levels were always lower in *WT* compared to *dcr1*Δ cells in subsequent periods. Importantly, we observed up to 3.5-fold changes between expression maxima and minima in *dcr1Δ* cells, which were always below 2-fold in *WT* cells. Thus, elevated temperatures induce high and oscillating expression of the *hsp104+* gene, which is dampened by Dcr1.

To investigate whether the repression of *hsp104+* mRNA levels by Dcr1 was also reflected at the protein level, we measured total fluorescence of cells expressing Hsp104-mCherry from the endogenous locus by spinning disk microscopy. This method allows monitoring Hsp104 levels with very high temporal resolution and, by measuring the intensity of several thousand individual cells, to assess variability within the population. Similar to the mRNA behavior, average Hsp104 protein levels were constantly higher and more oscillating in *dcr1Δ* cells than in *WT* cells (Figure 7B).

Together, these results further support our model that, under elevated temperatures, Hsp104 disaggregates cytoplasmic Dcr1, which can then return to the nucleus and maintain repression of both centromeric repeats and BANC genes. It also

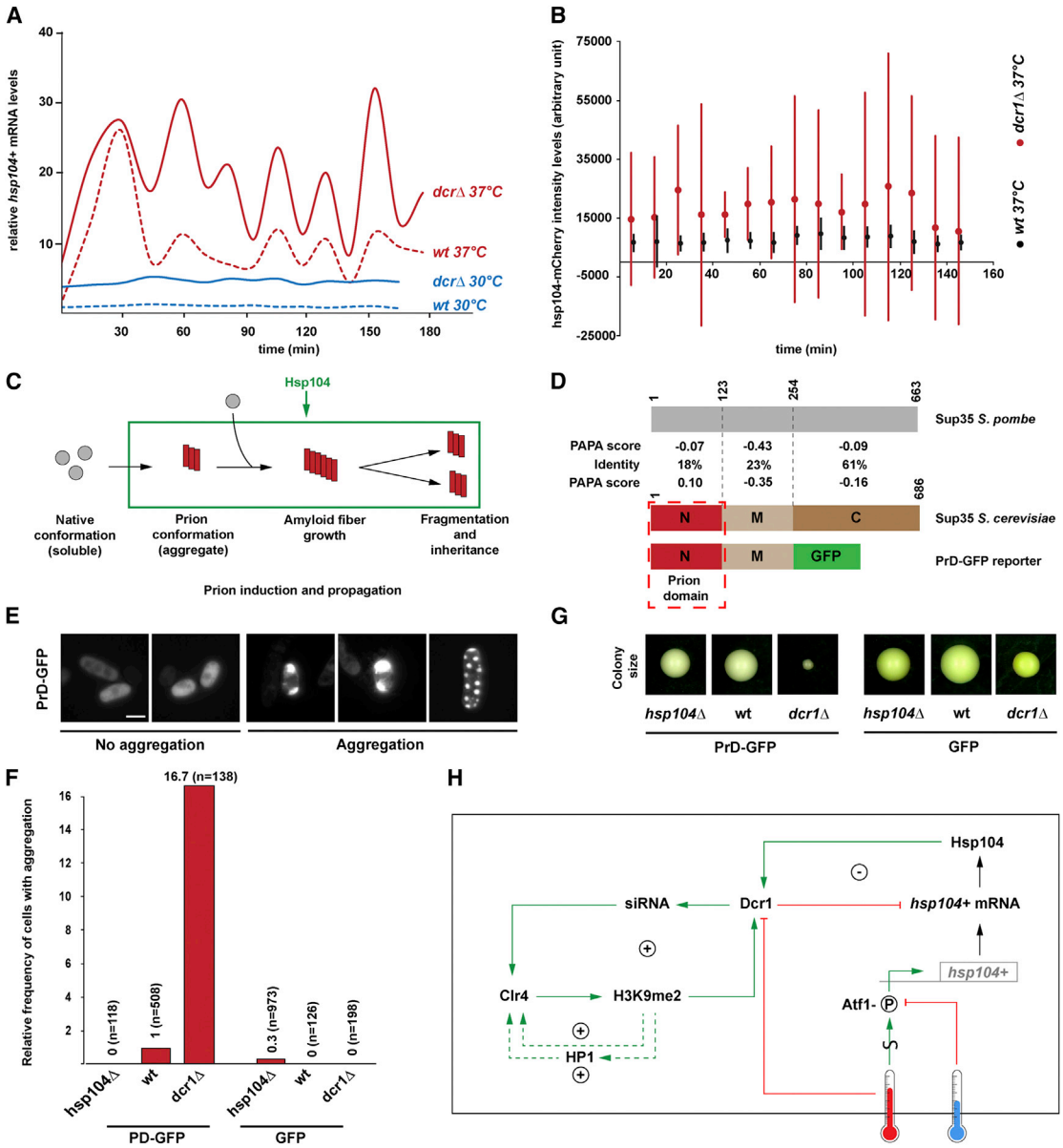

Figure 7. Dcr1 Inhibits Aggregation and Toxicity of a Prion Reporter

(A) *hsp104+* RNA levels measured every 15 min by quantitative RT-PCR in *WT* and *dcr1Δ* cells at 30°C or after shifting to 37°C.

(B) Hsp104-mCherry fluorescence levels in *WT* and *dcr1Δ* cells exposed to 37°C. Mean intensities of individual cells were measured. Averages of 10 min bins and SDs are shown.

(C) Schematic of prion induction and propagation.

(D) Domain architecture of *S. cerevisiae* Sup35, the PrD-GFP reporter used in (E)–(G) and *S. pombe* Sup35. Amino acid homology of individual domains was calculated using EMBOSS Needle, whereas prion forming propensity was calculated using the PAPA algorithm (Toombs et al., 2012).

(E) Examples of nonaggregating and aggregating phenotypes observed in different strains expressing PrD-GFP. The scale bar represents 5 μm.

(F) Frequency of aggregation in PrD-GFP- and GFP-expressing cells at 37°C (*WT*, *hsp104Δ*, and *dcr1Δ*), relative to the frequency observed in *WT* PrD-GFP-expressing cells.

(G) Colonies of PrD-GFP- and GFP-expressing strains showing strongly reduced growth in *dcr1Δ* PrD-GFP-transformed cells.

(H) Model for the formation of constitutive heterochromatin. The integration of multiple feedback motifs confers robustness to the system and buffers environmental insults. Red, >34°C; blue, <34°C. S depicts unknown oscillator; P indicates phosphorylation of Atf1.

reveals a negative feedback regulatory circuit in Dcr1-mediated control of *hsp104+* gene expression: whereas Dcr1 negatively regulates *hsp104+* expression, the Hsp104 protein positively regulates Dcr1 by keeping it in an active state.

Dcr1 Is Required to Repress Aggregation and Toxicity of a Prionogenic Protein

The forgoing results suggest that controlling the dynamics of BANC gene expression under constant thermal stress may serve

as a vital buffer to prevent potentially deleterious fluctuations in heat shock gene expression. Intriguingly, in addition to its role in protein disaggregation, Hsp104 plays a crucial role in prion formation, propagation, and elimination (Figure 7C). Whereas absence of Hsp104 prevents prion formation, too high levels lead to prion curing (Chernoff et al., 1995; Shorter and Lindquist, 2004). Thus, unsteady Hsp104 levels may favor prion occurrence, and it is therefore tempting to speculate that Dcr1-mediated dampening of oscillatory *hsp104+* expression might antagonize prion formation in *S. pombe*.

To determine the rate at which prionogenic proteins might switch to the prion conformation in *S. pombe*, we exploited a widely used GFP reporter containing the prion-forming domain (PrD) of *S. cerevisiae* Sup35 (Figure 7D), one of the most well-studied fungal prions (Tessier and Lindquist, 2009; Tyedmers et al., 2010b). We transformed *WT*, *dcr1Δ*, and *hsp104Δ* cells with plasmids encoding either the PrD-GFP construct or GFP alone and monitored fluorescence localization after growth at 37°C. *WT*, *dcr1Δ*, and *hsp104Δ* cells expressing the control plasmid showed limited or no aggregation, with most or all of the cells showing diffuse staining. In contrast, PrD-GFP aggregation was significantly higher in *dcr1Δ* cells (Figure 7F) than in *WT* or *hsp104Δ* cells, revealing a link between Dcr1 and aggregation of prionogenic proteins. PrD-GFP also appeared to be toxic to *dcr1Δ* cells, as they formed much smaller colonies than *dcr1+* and *dcr1Δ* cells transformed with PrD-GFP and GFP, respectively, and could not be further expanded (Figure 7G). Both *WT* and *dcr1Δ* cells showed aggregation of PrD-GFP in different patterns, including multiple dots distributed in the cytoplasm or one single region of aggregation (Figure 7E). These patterns are typical of the switch to the prion conformation. PrD-GFP aggregation was not observed in *hsp104Δ* cells. Thus, the *S. cerevisiae* PrD forms stable aggregates and is highly toxic when expressed in *S. pombe* cells that lack Dcr1.

Although definite proof that the PrD-GFP forms a bona fide prion in *S. pombe* demands further study, our results suggest that Dcr1-mediated dampening of oscillatory expression of *hsp104+* and possibly other BANC genes might have evolved to counteract prion induction and propagation that might otherwise be toxic for the cell.

DISCUSSION

This study highlights the remarkably strong and stable repressive activity of constitutive heterochromatin, uncovers a central role for Hsp104 in buffering environmentally induced epigenetic variation, and reveals an unanticipated role for Dcr1 in averting toxic aggregation of a prionogenic protein. Below, we speculate about the physiological relevance of feedback regulation of Dcr1 and Hsp104 and discuss the implications of our findings for our understanding of RNAi-mediated heterochromatin formation and epigenetic robustness.

Recycling of Aggregated Dcr1 in a Specialized Cytoplasmic Compartment

Using CLEM, we discovered that Dcr1 colocalizes with Hsp104 in membrane-free, electron-dense, cytoplasmic inclusions at elevated temperatures. SBEM imaging and subsequent 3D reconstruction revealed the existence of one such inclusion per cell during prolonged heat, generally localizing at the cellular periphery in the vicinity of vacuoles. We never observed these structures adjacent to the nuclear membrane, and their formation required thermal stress. Interestingly, we observed a high number of small cytoplasmic Dcr1 foci during acute temperature stress, which then clustered into one large inclusion after 3 hr and subsequently disappeared progressively, indicating that formation and disintegration of these misfolded protein inclusions are both active processes. Furthermore, FRAP experiments revealed that the Dcr1 proteins in these inclusions are immobile, consistent with this compartment containing aggregated proteins.

These features are reminiscent of cytosolic protein quality-control compartments that have been described in *S. cerevisiae* and mammalian cells such as the Q bodies (Escusa-Toret et al., 2013) or the insoluble protein deposit (IPOD) (Kaganovich et al., 2008). Q bodies also contain misfolded proteins and arise in response to a temperature increase, first as several small puncta that then fuse within 30 min into few larger foci. However, proteins in Q bodies are destined for degradation. Moreover, Q bodies remain as multiple small puncta, do not coalesce in fewer bigger foci, and rapidly disappear in *hsp104Δ* cells. Dcr1 bodies instead increase in size and persist in the absence of Hsp104. Accumulation of misfolded proteins in the IPOD compartment and colocalization with Hsp104 has also been shown to be typical for stress conditions in *S. cerevisiae* (Kaganovich et al., 2008). However, it is not known whether protein disaggregation is also taking place in IPODs. Rather, it is generally assumed that IPODs contain terminally aggregated proteins (Tyedmers et al., 2010a).

Our results imply that the inclusions that form in *S. pombe* in response to acute temperature stress are not simply sequestering protein aggregates that might otherwise be toxic for the cell but are rather functional compartments in which Hsp104 exerts its functions. We show that Hsp104 actively participates in the disaggregation of proteins in this cytoplasmic compartment. As exemplified by Dcr1, these proteins are not destined for proteolysis but are rather recycled. As suggested for IPOD in budding yeast, this compartment in *S. pombe* may serve a protective function by spatially sequestering protein aggregates from the site where most proteasomal degradation takes place (Tyedmers et al., 2010a). Therefore, we propose that the large protein inclusion that forms at elevated temperatures in fission yeast constitutes a major site of protein disaggregation under acute temperature stress and serves to maintain protein homeostasis by recycling misfolded proteins.

Toxic Aggregation of Prionogenic Proteins

Prions are proteins that can exist in a soluble functional form or as amyloid fibrils. The amyloid form of prions is a self-perpetuating conformation and thus acts as a protein-based element of heredity (Shorter and Lindquist, 2005). In *S. cerevisiae*, numerous proteins are capable of forming prions that stably propagate the altered protein conformation and associated phenotypes (Alberti et al., 2009). However, there have been no reports of prion formation in *S. pombe*.

Hsp104 plays an important role in the propagation of the amyloid prion conformation in *S. cerevisiae*. It shears amyloid

fibers to generate prion "seeds" or "propagons," which facilitates the inheritance of the prion state from generation to generation (Chernoff et al., 1995). In this respect, negative feedback regulation of *hsp104*+ and Dcr1 in *S. pombe* is fascinating, as it may constitute a homeostatic control mechanism that controls endogenous prion induction and propagation. Although definite proof has yet to be obtained, this hypothesis is supported by the highly increased frequency of aggregation that we observed for the exogenous PrD-GFP prion reporter in *dcr1*Δ cells. Interestingly, this aggregation is highly toxic. In contrast to *S. cerevisiae* Hsp104, *S. pombe* Hsp104 has been shown to support induction and propagation, but not curing of prions when expressed in *S. cerevisiae* (Reidy et al., 2013). It is therefore possible that PrD-GFP indeed forms prions in *dcr1Δ* cells. Because these cannot be cured in *S. pombe*, this could result in uncontrolled and irreversible propagation of aggregates, which has detrimental effects for the cell. Notably, endogenous prions have not yet been found and the number of putative prions predicted for *S. pombe* is significantly lower than for other fungi (Espinosa Angarica et al., 2013; Harrison et al., 2007). It is possible that the inability of *S. pombe* to cope with prionogenic proteins resulted in negative selection on prions while positively selecting Dcr1/Hsp104 feedback regulation.

PrD-GFP toxicity observed in this study is reminiscent of neurodegenerative diseases that share features with fungal proteins. Similar to β-sheet-rich amyloid fibrils formed by prions, many of the proteins involved in neurodegenerative conditions are deposited in insoluble, neurotoxic amyloid deposits, such as Aβ amyloid plaques in Alzheimer's disease or Lewy bodies in Parkinson's disease (Fraser, 2014; Halliday et al., 2014; Prusiner, 2012). *S. pombe* may therefore become an interesting model organism for studying detrimental prion-like protein aggregation in the future.

Transmission of an Epigenetic State through Successive Cell Divisions

A remarkable phenotype of *hsp104Δ* cells is that the *otr1*::*ade6*+-*on* epiallele can be stably maintained for more than 30 mitotic divisions, even in the absence of the stress that induced the epigenetic switch, and although normal Dcr1 distribution and BANC silencing are quickly re-established after stress removal. Thus, the descendants of the switching cells "remember" the chromatin state of the mother cell. This is reminiscent of inheritance of stress-induced disruption of heterochromatin in *Drosophila melanogaster*. When fly embryos are exposed to heat stress over multiple generations, the euchromatic chromatin state can be maintained over multiple successive generations before gradually returning to the normal state (Seong et al., 2011). The mechanism of this transgenerational inheritance of stress-induced heterochromatin disruption is unknown, and it is possible that the disrupted heterochromatin state is propagated actively. Similarly, we cannot rule out the possibility that the euchromatic state of the *otr1*::*ade6-on* epiallele is propagated by an active mechanism. However, rather than an active "memory" of the euchromatic state, we favor the idea that the long-lasting loss of *otr1*::*ade6*+ repression reflects an inherent difficulty to establish heterochromatin de novo by siRNAs in the absence of preexisting H3K9 methylation. This hypothesis is consistent with various attempts to artificially induce the formation of ectopic heterochromatin by either siRNAs or tethering of the RNAi machinery to nascent transcripts, which are inefficient processes (Bühler et al., 2006; Iida et al., 2008).

Once re-established, the *otr1*::*ade6-off* epiallele is again mitotically remarkably stable under nonstressful conditions, even in *hsp104*Δ cells. Similarly, cells that are able to establish heterochromatin upon artificial tethering of the RNAi machinery to nascent transcripts stably propagate the repressed state through mitosis (Bühler et al., 2006). These results are in accordance with a model in which RNAi functions cooperatively with parentally inherited H3K9 methylated histones to re-establish heterochromatin following DNA replication. During replication of heterochromatin, the RNA-induced transcriptional silencing (RITS) complex can bind to chromatin cooperatively via siRNA-mediated base pairing with nascent transcripts and association with parental H3K9me2-marked nucleosomes. RITS-mediated recruitment of Clr4 then guarantees methylation of the newly deposited histones and thus transmission of heterochromatin from interphase to interphase (Moazed, 2011).

Stabilization of Constitutive Heterochromatin by Nested Feedback Loops

The observations discussed above exemplify the importance of positive feedback in building up epigenetic memory (Ptashne, 2013). For chromatin modifications, positive feedback can arise if nucleosomes carrying a particular modification recruit enzymes that catalyze the same modification on proximal histone tails. Therefore, methylated H3K9 could recruit the methyltransferase Clr4 directly through binding to the chromodomain or indirectly via the chromodomains of HP1 proteins or the RITS complex. However, these positive feedback loops are not sufficient to maintain heterochromatin by themselves, and it has become apparent that they must collaborate with the RNAi pathway to lock the heterochromatic state of centromeric repeats (Moazed, 2011). Therefore, we propose a model for the formation of constitutive heterochromatin that implies the integration of multiple feedback motifs to achieve robustness (Figure 7H).

In our model, Dcr1 constitutes a sensitive regulatory step that can respond to temperature changes. Without Hsp104, this step becomes ultrasensitive to thermal stress and inactivation of Dcr1 by elevated temperatures can trigger a bistable epigenetic switch. Importantly, among other factors that are required for heterochromatin repression in *S. pombe*, Hsp104 is unusual in the sense that its absence does not show complete penetrance. This suggests that the other positive feedback loops function partially redundant or that mild temperature stress inactivates Dcr1 only partly. Furthermore, switching to a euchromatic state may only occur if siRNA levels drop below a critical threshold. Thus, bistability of centromeric heterochromatin in *hsp104Δ* cells may also considerably depend on the half-life of centromeric siRNAs.

Our model predicts a concerted action of several positive feedback loops that guarantees the inheritance of the constitutive heterochromatic state of centromeric repeat sequences.

The model also highlights the importance of temperature-induced transcription of *hsp104+*, which is required for proper functioning of RNAi. But what is the role of negative regulation of *hsp104+* expression by Dcr1? Positive feedback can implement irreversible bistable switches that may only be forced back to the alternate state if coupled to negative feedback (Brandman and Meyer, 2008). Thus, negative feedback regulation of Dcr1 and *hsp104+* may have been integrated into the positive feedback core to still confer plasticity to the system. Alternatively, other processes such as the aforementioned regulation of prion induction and propagation may have been the driving force for the evolution of this negative feedback loop.

CONCLUSION

We discovered that mutating *hsp104+* predisposes *S. pombe* to undergo temperature-induced, heritable changes in heterochromatic gene expression. Although Dcr1 is certainly not the only client of Hsp104, our results strongly suggest that the bistability of centromeric heterochromatin in *hsp104Δ* cells is causally linked to malfunctioning Dcr1. Future studies with *hsp104+* mutants could reveal much hidden epigenetic variation that may or may not be linked to noncoding RNA metabolism. Similarly, Dcr1-deficient cells may enable the discovery and further characterization of endogenous prions in *S. pombe.* Finally, we hope that our proposed regulatory network model sparks future efforts to study the dynamics of the suggested feedback motifs. Combined with mathematical modeling approaches, we are convinced that this will significantly increase our understanding of epigenetic memory.

EXPERIMENTAL PROCEDURES

Extended procedures are described in the Supplemental Information.

Strains and Plasmids

S. pombe strains and plasmids used are described in the Supplemental Information.

Silencing Assays

Serial 10-fold dilutions of the strains indicated were plated on YES or YE plates and grown at the temperatures indicated. To score phenotype of individual colonies, 250–500 cells/plate were spotted and colonies were automatically counted using Matlab (MathWorks).

CLEM

Cells were prepared similar to Kukulski et al. (2011). Shortly, cells were high-pressure frozen, freeze substituted, and embedded in HM20 resin. One hundred to two hundred nanometer ultrathin sections were cut and imaged with a wide-field fluorescence microscope or spinning disk microscope, followed by transmission EM. Images were correlated with TrakEM.

SBEM

Fixed cells were prepared according to the rOTO NCMIR protocol. Embedded blocks were imaged with 3View (GATAN) in a scanning EM. Cells were digitally reconstructed using TrakEM (Fiji).

Live Fluorescence Microscopy and FRAP

S. pombe cells were imaged on agarose patches with a spinning disk microscope. For time-lapse experiments, cells were kept in culture and aliquots were taken at different time points. Intensity and volume measurement of foci was done with ImageJ. FRAP was performed on cells mounted on a Ludin chamber using a 473 nm laser.

Immunofluorescence

Synchronized cells were fixed, spheroblasted, and stained with anti-Tat1 antibody. Cells were imaged with a wide-field fluorescence microscope.

Gene Expression Analysis and Chromatin Immunoprecipitation

RNA isolation, cDNA synthesis, and quantitative RT-PCR were performed as previously described (Emmerth et al., 2010). Chromatin immunoprecipitation (ChIP) was performed as described in Bühler et al. (2006) using 2.5 μg of an antibody against dimethylated H3K9 (Kimura et al., 2008). Primers are listed in Table S3.

Generation of Small RNA Libraries for High-Throughput Sequencing

Sample libraries were prepared and analyzed as in the Supplemental Information. siRNAs were defined as reads with a decrease in number of reads of at least 8-fold between WT cells and Dcr1Δ cells.

ACCESSION NUMBERS

Deep sequencing data were deposited to the NCBI Gene Expression Omnibus and are available under accession number GSE60640.

SUPPLEMENTAL INFORMATION

Supplemental Information includes Supplemental Discussion, Supplemental Experimental Procedures, three figures, three tables, and two movies and can be found with this article online at http://dx.doi.org/10.1016/j.celrep.2014.12.006.

AUTHOR CONTRIBUTIONS

M.B. and D.O. conceived and designed the experiments. D.O. performed most of the experiments. A.B. performed phenotypic characterization and RNA measurements. M.A.K. wrote scripts for automated colony counting and fluorescence measurement. C.G. performed SBEM imaging. R.S. performed FRAP experiments. Y.S. performed ChIP experiments. M.B. obtained funding and oversaw the study. M.B. and D.O. wrote the manuscript.

ACKNOWLEDGMENTS

We thank Prof. Henning Stahlberg (C-CINA, Biozentrum, University of Basel) for sharing equipment and Jens Tyedmers for sharing reagents and for valuable discussions. We are grateful to Christopher Bleck for help with EM sample preparation, to Hans-Rudolf Hotz for bioinformatics support, to Wanda Kukulski for technical advices on CLEM, and to Kirsten Jacobeit for library preparation. This work was supported by funds from the European Research Council (280410). The Friedrich Miescher Institute for Biomedical Research is supported by the Novartis Research Foundation.

Received: August 18, 2014
Revised: November 6, 2014
Accepted: December 2, 2014
Published: December 24, 2014

REFERENCES

Alberti, S., Halfmann, R., King, O., Kapila, A., and Lindquist, S. (2009). A systematic survey identifies prions and illuminates sequence features of prionogenic proteins. Cell *137*, 146–158.

Allshire, R.C. (1995). Elements of chromosome structure and function in fission yeast. Semin. Cell Biol. *6*, 55–64.

Allshire, R.C., Javerzat, J.P., Redhead, N.J., and Cranston, G. (1994). Position effect variegation at fission yeast centromeres. Cell *76*, 157–169.

Anderson, P., and Kedersha, N. (2006). RNA granules. J. Cell Biol. *172*, 803–808.

Barraud, P., Emmerth, S., Shimada, Y., Hotz, H.-R., Allain, F.H.-T., and Bühler, M. (2011). An extended dsRBD with a novel zinc-binding motif mediates nuclear retention of fission yeast Dicer. EMBO J. *30*, 4223–4235.

Brandman, O., and Meyer, T. (2008). Feedback loops shape cellular signals in space and time. Science *322*, 390–395.

Bühler, M., Verdel, A., and Moazed, D. (2006). Tethering RITS to a nascent transcript initiates RNAi- and heterochromatin-dependent gene silencing. Cell *125*, 873–886.

Castel, S.E., and Martienssen, R.A. (2013). RNA interference in the nucleus: roles for small RNAs in transcription, epigenetics and beyond. Nat. Rev. Genet. *14*, 100–112.

Chernoff, Y.O., Lindquist, S.L., Ono, B., Inge-Vechtomov, S.G., and Liebman, S.W. (1995). Role of the chaperone protein Hsp104 in propagation of the yeast prion-like factor [psi+]. Science *268*, 880–884.

Chikashige, Y., Kinoshita, N., Nakaseko, Y., Matsumoto, T., Murakami, S., Niwa, O., and Yanagida, M. (1989). Composite motifs and repeat symmetry in S. pombe centromeres: direct analysis by integration of NotI restriction sites. Cell *57*, 739–751.

Denk, W., and Horstmann, H. (2004). Serial block-face scanning electron microscopy to reconstruct three-dimensional tissue nanostructure. PLoS Biol. *2*, e329.

DeSantis, M.E., Leung, E.H., Sweeny, E.A., Jackrel, M.E., Cushman-Nick, M., Neuhaus-Follini, A., Vashist, S., Sochor, M.A., Knight, M.N., and Shorter, J. (2012). Operational plasticity enables hsp104 to disaggregate diverse amyloid and nonamyloid clients. Cell *151*, 778–793.

Doyle, S.M., Genest, O., and Wickner, S. (2013). Protein rescue from aggregates by powerful molecular chaperone machines. Nat. Rev. Mol. Cell Biol. *14*, 617–629.

Dunand-Sauthier, I., Walker, C., Wilkinson, C., Gordon, C., Crane, R., Norbury, C., and Humphrey, T. (2002). Sum1, a component of the fission yeast eIF3 translation initiation complex, is rapidly relocalized during environmental stress and interacts with components of the 26S proteasome. Mol. Biol. Cell *13*, 1626–1640.

Ekwall, K., Cranston, G., and Allshire, R.C. (1999). Fission yeast mutants that alleviate transcriptional silencing in centromeric flanking repeats and disrupt chromosome segregation. Genetics *153*, 1153–1169.

Emmerth, S., Schober, H., Gaidatzis, D., Roloff, T., Jacobeit, K., and Bühler, M. (2010). Nuclear retention of fission yeast dicer is a prerequisite for RNAi-mediated heterochromatin assembly. Dev. Cell *18*, 102–113.

Escusa-Toret, S., Vonk, W.I.M., and Frydman, J. (2013). Spatial sequestration of misfolded proteins by a dynamic chaperone pathway enhances cellular fitness during stress. Nat. Cell Biol. *15*, 1231–1243.

Espinosa Angarica, V., Ventura, S., and Sancho, J. (2013). Discovering putative prion sequences in complete proteomes using probabilistic representations of Q/N-rich domains. BMC Genomics *14*, 316.

Feil, R., and Fraga, M.F. (2011). Epigenetics and the environment: emerging patterns and implications. Nat. Rev. Genet. *13*, 97–109.

Fraga, M.F., Ballestar, E., Paz, M.F., Ropero, S., Setien, F., Ballestar, M.L., Heine-Suñer, D., Cigudosa, J.C., Urioste, M., Benitez, J., et al. (2005). Epigenetic differences arise during the lifetime of monozygotic twins. Proc. Natl. Acad. Sci. USA *102*, 10604–10609.

Fraser, P.E. (2014). Prions and prion-like proteins. J. Biol. Chem. *289*, 19839–19840.

Fujita, K., Kawai, R., Iwahashi, H., and Komatsu, Y. (1998). Hsp104 responds to heat and oxidative stress with different intracellular localization in Saccharomyces cerevisiae. Biochem. Biophys. Res. Commun. *248*, 542–547.

Glover, J.R., and Lindquist, S. (1998). Hsp104, Hsp70, and Hsp40: a novel chaperone system that rescues previously aggregated proteins. Cell *94*, 73–82.

Goldberg, A.L. (2003). Protein degradation and protection against misfolded or damaged proteins. Nature *426*, 895–899.

Gottschling, D.E. (2004). Summary: epigenetics—from phenomenon to field. Cold Spring Harb. Symp. Quant. Biol. *69*, 507–519.

Grossniklaus, U., Kelly, W.G., Ferguson-Smith, A.C., Pembrey, M., and Lindquist, S. (2013). Transgenerational epigenetic inheritance: how important is it? Nat. Rev. Genet. *14*, 228–235.

Halliday, M., Radford, H., and Mallucci, G.R. (2014). Prions: generation and spread versus neurotoxicity. J. Biol. Chem. *289*, 19862–19868.

Harrison, L.B., Yu, Z., Stajich, J.E., Dietrich, F.S., and Harrison, P.M. (2007). Evolution of budding yeast prion-determinant sequences across diverse fungi. J. Mol. Biol. *368*, 273–282.

Holoch, D., and Moazed, D. (2012). RNAi in fission yeast finds new targets and new ways of targeting at the nuclear periphery. Genes Dev. *26*, 741–745.

Iida, T., Nakayama, J., and Moazed, D. (2008). siRNA-mediated heterochromatin establishment requires HP1 and is associated with antisense transcription. Mol. Cell *31*, 178–189.

Kaganovich, D., Kopito, R., and Frydman, J. (2008). Misfolded proteins partition between two distinct quality control compartments. Nature *454*, 1088–1095.

Kawai, R., Fujita, K., Iwahashi, H., and Komatsu, Y. (1999). Direct evidence for the intracellular localization of Hsp104 in Saccharomyces cerevisiae by immunoelectron microscopy. Cell Stress Chaperones *4*, 46–53.

Kimura, H., Hayashi-Takanaka, Y., Goto, Y., Takizawa, N., and Nozaki, N. (2008). The organization of histone H3 modifications as revealed by a panel of specific monoclonal antibodies. Cell Struct. Funct. *33*, 61–73.

Kloc, A., Zaratiegui, M., Nora, E., and Martienssen, R. (2008). RNA interference guides histone modification during the S phase of chromosomal replication. Curr. Biol. *18*, 490–495.

Kon, N., Krawchuk, M.D., Warren, B.G., Smith, G.R., and Wahls, W.P. (1997). Transcription factor Mts1/Mts2 (Atf1/Pcr1, Gad7/Pcr1) activates the M26 meiotic recombination hotspot in Schizosaccharomyces pombe. Proc. Natl. Acad. Sci. USA *94*, 13765–13770.

Kukulski, W., Schorb, M., Welsch, S., Picco, A., Kaksonen, M., and Briggs, J.A.G. (2011). Correlated fluorescence and 3D electron microscopy with high sensitivity and spatial precision. J. Cell Biol. *192*, 111–119.

Lawrence, C.L., Maekawa, H., Worthington, J.L., Reiter, W., Wilkinson, C.R.M., and Jones, N. (2007). Regulation of Schizosaccharomyces pombe Atf1 protein levels by Sty1-mediated phosphorylation and heterodimerization with Pcr1. J. Biol. Chem. *282*, 5160–5170.

Micheva, K.D., and Smith, S.J. (2007). Array tomography: a new tool for imaging the molecular architecture and ultrastructure of neural circuits. Neuron *55*, 25–36.

Moazed, D. (2011). Mechanisms for the inheritance of chromatin states. Cell *146*, 510–518.

Mollet, S., Cougot, N., Wilczynska, A., Dautry, F., Kress, M., Bertrand, E., and Weil, D. (2008). Translationally repressed mRNA transiently cycles through stress granules during stress. Mol. Biol. Cell *19*, 4469–4479.

Parsell, D.A., Kowal, A.S., Singer, M.A., and Lindquist, S. (1994). Protein disaggregation mediated by heat-shock protein Hsp104. Nature *372*, 475–478.

Prusiner, S.B. (2012). Cell biology. A unifying role for prions in neurodegenerative diseases. Science *336*, 1511–1513.

Ptashne, M. (2013). Epigenetics: core misconcept. Proc. Natl. Acad. Sci. USA *110*, 7101–7103.

Reidy, M., Sharma, R., and Masison, D.C. (2013). Schizosaccharomyces pombe disaggregation machinery chaperones support Saccharomyces cerevisiae growth and prion propagation. Eukaryot. Cell *12*, 739–745.

Sanchez, Y., and Lindquist, S.L. (1990). HSP104 required for induced thermotolerance. Science *248*, 1112–1115.

Seong, K.-H., Li, D., Shimizu, H., Nakamura, R., and Ishii, S. (2011). Inheritance of stress-induced, ATF-2-dependent epigenetic change. Cell *145*, 1049–1061.

Shorter, J., and Lindquist, S. (2004). Hsp104 catalyzes formation and elimination of self-replicating Sup35 prion conformers. Science *304*, 1793–1797.

Shorter, J., and Lindquist, S. (2005). Prions as adaptive conduits of memory and inheritance. Nat. Rev. Genet. *6*, 435–450.

Song, J., Irwin, J., and Dean, C. (2013). Remembering the prolonged cold of winter. Curr. Biol. *23*, R807–R811.

Tessier, P.M., and Lindquist, S. (2009). Unraveling infectious structures, strain variants and species barriers for the yeast prion [PSI+]. Nat. Struct. Mol. Biol. *16*, 598–605.

Toombs, J.A., Petri, M., Paul, K.R., Kan, G.Y., Ben-Hur, A., and Ross, E.D. (2012). De novo design of synthetic prion domains. Proc. Natl. Acad. Sci. USA *109*, 6519–6524.

Tyedmers, J., Mogk, A., and Bukau, B. (2010a). Cellular strategies for controlling protein aggregation. Nat. Rev. Mol. Cell Biol. *11*, 777–788.

Tyedmers, J., Treusch, S., Dong, J., McCaffery, J.M., Bevis, B., and Lindquist, S. (2010b). Prion induction involves an ancient system for the sequestration of aggregated proteins and heritable changes in prion fragmentation. Proc. Natl. Acad. Sci. USA *107*, 8633–8638.

Vashist, S., Cushman, M., and Shorter, J. (2010). Applying Hsp104 to protein-misfolding disorders. Biochem. Cell Biol. *88*, 1–13.

Volpe, T.A., Kidner, C., Hall, I.M., Teng, G., Grewal, S.I.S., and Martienssen, R.A. (2002). Regulation of heterochromatic silencing and histone H3 lysine-9 methylation by RNAi. Science *297*, 1833–1837.

Volpe, T., Schramke, V., Hamilton, G.L., White, S.A., Teng, G., Martienssen, R.A., and Allshire, R.C. (2003). RNA interference is required for normal centromere function in fission yeast. Chromosome Res. *11*, 137–146.

Wong, C.C.Y., Caspi, A., Williams, B., Craig, I.W., Houts, R., Ambler, A., Moffitt, T.E., and Mill, J. (2010). A longitudinal study of epigenetic variation in twins. Epigenetics *5*, 516–526.

Woolcock, K.J., Gaidatzis, D., Punga, T., and Bühler, M. (2011). Dicer associates with chromatin to repress genome activity in Schizosaccharomyces pombe. Nat. Struct. Mol. Biol. *18*, 94–99.

Woolcock, K.J., Stunnenberg, R., Gaidatzis, D., Hotz, H.-R., Emmerth, S., Barraud, P., and Bühler, M. (2012). RNAi keeps Atf1-bound stress response genes in check at nuclear pores. Genes Dev. *26*, 683–692.